Pergamon

Int. J. Mech. Sci. Vol. 39, No. 7, pp. 841–857, 1997

0020-7403/97 $17.00 + 0.00

PII:S0020-7403(96)00078-1

IDENTIFICATION OF THE UNBALANCE DISTRIBUTION IN FLEXIBLE ROTORS

YUAN-PIN SHIH and AN-CHEN LEE

Department of Mechanical Engineering, National Chiao Tung University, Taiwan, Republic of China

(*Received* 10 *February* 1995; *in revised form* 12 *April* 1996)

Abstract—This paper presents a new method for estimating unbalance distributions of flexible shafts and constant eccentricities of rigid disks based on the transfer matrix method for analyzing the steady-state responses of rotor-bearing systems, in which the transfer matrix of a flexible shaft is derived in a continuous sense with any spatial unbalance distribution. Rotary inertia, gyroscopic and transverse-shear effects are also included. When deflections and deflection angles of one free end are measurable, the unbalance distribution of shafts and disks can be estimated under operating conditions by the proposed method. The main advantage of this identification technique is that only the state vector of the one free end of the rotating shaft need to be measured. Justification of the method is presented by numerical simulations. © 1997 Elsevier Science Ltd. All rights reserved.

Keywords: flexible rotor, unbalance identification.

NOTATION

A, D_f, ρ	cross-section area, diameter and density of the shaft
E, G, K_s	Young's modulus, shear modulus and shear factor
I, J	transverse and polar area moment of inertia of the shaft
L	length of the shaft segment
M, Q	bending moment and shear force
P, T	axial force and torque acting on the shaft
e, e_{dx}, e_{dy}	eccentricity of the disk and projections, respectively, in X and Y directions
$r(Z), r_x(Z), r_y(Z)$	eccentricity of the shaft and projections, respectively, in X and Y directions
X, Y	deflection in X and Y directions of fixed coordinates XYZ
Z, t	position and time coordinates, respectively
α, β	slope in the XZ and YZ planes
ϕ	angular position of shaft unbalance in moving coordinates
ω	rotating speed
n	the number of the term in Fourier series
m	the number of the shaft with unbalance distribution
q	the number of the disk with unbalance eccentricity
k	the number of rotating speed
m_1	the number of parameters in unbalance distribution

Subscripts and superscripts

b, t	caused by bending moment, shear force
c, s	associated to cosine, sine terms
h, p	homogeneous solution, particular solution
r, l	right, left
x, y	components in X and Y directions
~	labeled for column vector
′	differentiation w.r.t. Z

INTRODUCTION

Rotor unbalance considered does not only cause vibration, it also transmits rotational forces to rotor bearings and to the supporting structure. The forces thus transmitted may damage the machine and shorten its working life. All rotors have residual unbalance during manufacturing because of machining tolerances and material inhomogeneity. Thus, it is necessary to balance these rotors, as carefully as possible, to ensure smooth running.

Over the years, two major balancing techniques have commonly been employed; the modal balancing method, and the influence coefficients method. The modal balancing technique was

developed by Bishop [1] and further investigated by several researchers, such as Kellenberger [2], Shimada and Miwa [3], Shimada and Fujisawa [4] and Saito and Azuna [5]. In this method, the critical speed mode shapes of the rotor must be known from either theoretical or experimental measurements. Also, mass distribution must also be determined from the geometry of the rotor. The accuracy of the method depends on the knowledge of the rotor mode shapes, which may become quite complex for modes higher than the second critical speed. The influence coefficients technique was presented by Goodman [6]. It has been improved and tested by several authors such as Lund and Tonneson [7], Tessarzik and Badgley [8], Tessarzik *et al.* [9, 10] and Everett [11], in the laboratory and acceptable balancing has been achieved. In general, this method requires an accurate measurement of vibration phase angle in order to produce acceptable results. Various field balancing methods have also been developed, as discussed in detail in Ehrich [12].

The subject of balancing has been of interest to users of rotating machinery and further study in the theory and practice of balancing is still going on. Intuitively, it seems clear that the best way to balance a rotor is first to find the unbalance distribution and then add weights at given radial distances from the axis of rotation to compensate for it. However, due to deficiencies in methods for finding unbalance distribution, the concept of dynamic testing has long been emphasized. Consequently, we may not obtain the best quality of balance.

The purpose of this paper is to present a method for estimating the unbalance distribution in flexible rotors. This article is an extension of the work of Lee [13], who first gave a complete analysis of a rotating shaft's continuous "state of unbalance". This method is based on the transfer matrix method (TMM) of analyzing the steady-state responses of rotor-bearing systems. The rotor-bearing systems considered here are composed of flexible shafts with spatial unbalance distributions, multiple rigid disks with constant eccentricities and linear bearings. Each bearing can be represented by eight linearized parameters, i.e. four stiffness and four damping coefficients. Since the system considered here is driven by an unbalanced force, the steady-state of the rotor will only contain a synchronous frequency component. The rationale of the method is described as below. By transforming any continuously distributed shaft unbalance function into its Fourier series representation, we can obtain the coefficients of the sine and cosine terms. Next, the overall transfer matrix including the shaft sections, bearings and disks is derived in terms of linear combinations of the unbalance parameters and the system parameters. Then, according to the boundary conditions, we formulate the normal equation by using the relations between these unknown coefficients and the known system parameters. Finally, identification can be realized from the simulated measured response data, i.e. the state variables of both displacements and angles measured at one free end in the shaft, induced by rotor unbalance using the least-squares method. The main advantage of this method is that only the states of one free end need to be measured, along with of course system parameters such as shaft geometry of shaft, material properties, rotating speed, bearing dynamic coefficients and so on. Justification of the method is given by numerical simulation.

EQUATIONS OF DISPLACEMENT FUNCTIONS FOR THE UNBALANCED SHAFT

In this section, the primary equations needed in this paper are given. For the detail derivation of them, the readers may refer to Lee *et al.* [13]. The governing equations of a rotating shaft considering the rotary inertia, gyroscopic, transverse shear effects and unbalance distribution can be derived as follows

$$\begin{aligned}
&\frac{\partial^4 X}{\partial Z^4} - \left(\frac{\rho}{K_s G} + \frac{\rho}{E}\right)\frac{\partial^4 X}{\partial Z^2 \partial t^2} + \frac{\rho^2}{K_s G E}\frac{\partial^4 X}{\partial t^4} + \frac{\rho A}{EI}\frac{\partial^2 X}{\partial t^2} \\
&\quad - \frac{2\rho\omega}{E}\left(\frac{\partial^3 Y}{\partial Z^2 \partial t} - \frac{\rho}{K_s G}\frac{\partial^3 Y}{\partial t^3}\right) - \frac{P}{EI}\frac{\partial^2 X}{\partial Z^2} - \frac{T\rho}{EIK_s G}\frac{\partial^3 Y}{\partial Z \partial t^2} \\
&\quad + \frac{T}{EI}\frac{\partial^3 Y}{\partial Z^3} = \frac{\rho \cdot A \cdot r(Z) \cdot \omega^2 \cdot \cos(\omega t + \phi)}{EI} - \frac{\rho \cdot r''(Z) \cdot \omega^2 \cdot \cos(\omega t + \phi)}{K_s G} \\
&\quad + \frac{\rho^2 \cdot r(Z) \cdot \omega^4 \cdot \cos(\omega t + \phi)}{K_s G E} - \frac{T \cdot r'(Z) \cdot \rho \cdot \omega^2 \cdot \sin(\omega t + \phi)}{K_s G E I}
\end{aligned} \tag{1}$$

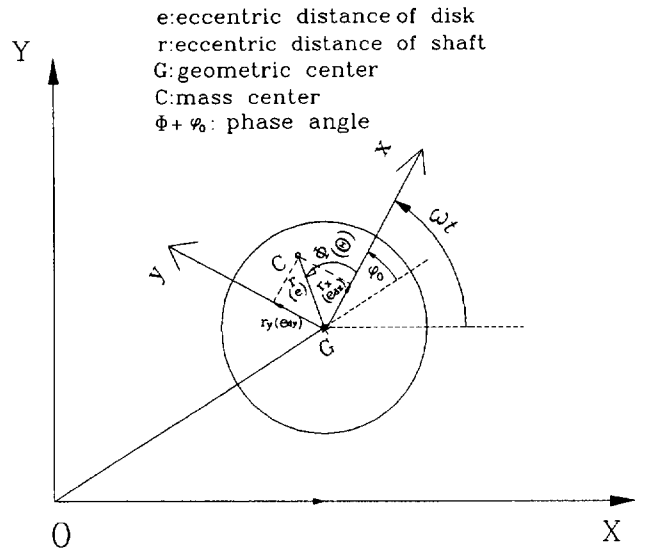

Fig. 1. Geometries of a rotating shaft (or a disk) with unbalance mass.

in XZ plane and

$$\frac{\partial^4 Y}{\partial Z^4} - \left(\frac{\rho}{K_s G} + \frac{\rho}{E}\right)\frac{\partial^4 Y}{\partial Z^2 \partial t^2} + \frac{\rho^2}{K_s G E}\frac{\partial^4 Y}{\partial t^4} + \frac{\rho A}{EI}\frac{\partial^2 Y}{\partial t^2} + \frac{2\rho\omega}{E}\left(\frac{\partial^3 X}{\partial Z^2 \partial t} - \frac{\rho}{K_s G}\frac{\partial^3 X}{\partial t^3}\right) - \frac{P}{EI}\frac{\partial^2 Y}{\partial Z^2} + \frac{T\rho}{EIK_s G}\frac{\partial^3 X}{\partial Z \partial t^2} - \frac{T}{EI}\frac{\partial^3 X}{\partial Z^3} = \frac{\rho \cdot A \cdot r(Z) \cdot \omega^2 \cdot \sin(\omega t + \phi)}{EI} - \frac{\rho \cdot r''(Z) \cdot \omega^2 \cdot \sin(\omega t + \phi)}{K_s G} + \frac{\rho^2 \cdot r(Z) \cdot \omega^4 \cdot \sin(\omega t + \phi)}{K_s G E} + \frac{T \cdot r'(Z) \cdot \rho \cdot \omega^2 \cdot \cos(\omega t + \phi)}{K_s G E I} \tag{2}$$

in YZ plane, where ϕ and $r(Z)$ are shown in Fig. 1.

Because the synchronous whirling orbit is elliptical in general, the steady-state solutions of the above two linear differential equations can be expressed as

$$X(Z, t) = X_c(Z)\cos\omega t + X_s(Z)\sin\omega t$$
$$Y(Z, t) = Y_c(Z)\cos\omega t + Y_s(Z)\sin\omega t \tag{3}$$

where X_c, X_s, Y_c and Y_s are the displacement functions of steady-state responses.

Since eccentricity function of shaft unbalance is assumed to be finite and piecewise continuous on each shaft section, its Fourier series representation can be uniquely determined, i.e.

$$r(Z) = r_0 + \sum_{n=1}^{\infty}\left[(r_c)_n \cos\frac{n\pi Z}{L} + (r_s)_n \sin\frac{n\pi Z}{L}\right]. \tag{4}$$

For the practical unbalance distribution of a rotor, convergence conditions (Wylie and Barret [14]) are always satisfied and would not cause any convergence problem. However, from the rigorously mathematical point of view, if the unbalance distribution does not converge at some points, the shaft can be cut at these points into several sections and then the solution can be obtained in a similar procedure.

Substituting Eqns (2) and (3) into Eqn (1) and separating the $\cos\omega t$ and $\sin\omega t$ terms, the four ordinary differential equations can be obtained. The general solutions of the displacement

function can be expressed into the sum of homogeneous and particular solutions as below.

$$\begin{aligned} X_c(Z) &= X_c^h + X_c^p \\ X_s(Z) &= X_s^h + X_s^p \\ Y_c(Z) &= Y_c^h + Y_c^p \\ Y_s(Z) &= Y_s^h + Y_s^p \end{aligned} \tag{5}$$

where the homogeneous solutions can be written as

$$\begin{aligned} X_c^h(Z) = &\sum_{i=1}^{4} A_i \cdot e^{a_i Z} \cdot \cos b_i Z + \sum_{i=5}^{8} A_i \cdot e^{a_i Z} \cdot \cos b_i Z \\ &- \sum_{i=1}^{4} B_i \cdot e^{a_i Z} \cdot \sin b_i Z + \sum_{i=5}^{8} B_i \cdot e^{a_i Z} \cdot \sin b_i Z \\ X_s^h(Z) = &\sum_{i=1}^{4} A_i \cdot e^{a_i Z} \cdot \sin b_i Z + \sum_{i=5}^{8} A_i \cdot e^{a_i Z} \cdot \sin b_i Z \\ &+ \sum_{i=1}^{4} B_i \cdot e^{a_i Z} \cdot \cos b_i Z - \sum_{i=5}^{8} B_i \cdot e^{a_i Z} \cdot \cos b_i Z \\ Y_c^h(Z) = &- \sum_{i=1}^{4} A_i \cdot e^{a_i Z} \cdot \sin b_i Z + \sum_{i=5}^{8} A_i \cdot e^{a_i Z} \cdot \sin b_i Z \\ &- \sum_{i=1}^{4} B_i \cdot e^{a_i Z} \cdot \cos b_i Z - \sum_{i=5}^{8} B_i \cdot e^{a_i Z} \cdot \cos b_i Z \\ Y_s^h(Z) = &\sum_{i=1}^{4} A_i \cdot e^{a_i Z} \cdot \cos b_i Z - \sum_{i=5}^{8} A_i \cdot e^{a_i Z} \cdot \cos b_i Z \\ &- \sum_{i=1}^{4} B_i \cdot e^{a_i Z} \cdot \sin b_i Z - \sum_{i=5}^{8} B_i \cdot e^{a_i Z} \cdot \sin b_i Z. \end{aligned} \tag{6}$$

The coefficients a_i and b_i are, respectively, the real and imaginary part of the characteristic values (details listed in Lee *et al.* [13]).

When ϕ = constant, the particular solutions can be expressed by

$$\begin{aligned} X_c^p &= \zeta_{10} + \sum_{n=1}^{\infty} \left(\mu_{cn}^c \cdot \cos \frac{n\pi Z}{L} + \mu_{cn}^s \cdot \sin \frac{n\pi Z}{L} \right) \\ X_s^p &= \zeta_{20} + \sum_{n=1}^{\infty} \left(\mu_{sn}^c \cdot \cos \frac{n\pi Z}{L} + \mu_{sn}^s \cdot \sin \frac{n\pi Z}{L} \right) \\ Y_c^p &= \zeta_{30} + \sum_{n=1}^{\infty} \left(v_{cn}^c \cdot \cos \frac{n\pi Z}{L} + v_{cn}^s \cdot \sin \frac{n\pi Z}{L} \right) \\ Y_s^p &= \zeta_{40} + \sum_{n=1}^{\infty} \left(v_{sn}^c \cdot \cos \frac{n\pi Z}{L} + v_{sn}^s \cdot \sin \frac{n\pi Z}{L} \right) \end{aligned} \tag{7}$$

where coefficients ζ, μ, v are listed in Appendix A of Lee *et al.* [13]. If the angular position of unbalance varies along the shaft due to the mass center of shaft in three-dimensional space, we can resolve $r(Z)$ into the components $r_x(z)$ and $r_y(z)$, respectively, in X and Y directions, with $\phi = 0°$ for $r_x(z)$ and $\phi = 90°$ for $r_y(z)$ for the shaft segment. Thus, we can obtain the particular solution of $\phi \neq$ constant by superposing those of $\phi = 0°$ for $r_x(Z)$ and $\phi = 90°$ for $r_y(Z)$ in the same manner as ϕ = constant.

Differentiating Eqn (4) to yield the relationships of the real constants A_i and B_i of displacement functions and their derivatives can be written in the following form

$$\{W\} = \begin{bmatrix} \mathbf{X}_c \\ \mathbf{X}_s \\ \mathbf{Y}_c \\ \mathbf{Y}_s \\ 1 \end{bmatrix} = \underset{17\times 17}{[F]} \begin{bmatrix} \mathbf{A} \\ \mathbf{B} \\ 1 \end{bmatrix} \tag{8}$$

where $\mathbf{X}_c = [X_c\ X_c'\ X_c''\ X_c''']^t$, $\mathbf{X}_s = [X_s\ X_s'\ X_s''\ X_s''']^t$, $\mathbf{Y}_c = [Y_c\ Y_c'\ Y_c''\ Y_c''']^t$, $\mathbf{Y}_s = [Y_s\ Y_s'\ Y_s''\ Y_s''']^t$, $\mathbf{A} = [A_1\ A_2\ A_3\ A_4\ A_5\ A_6\ A_7\ A_8]^t$, $\mathbf{B} = [B_1\ B_2\ B_3\ B_4\ B_5\ B_6\ B_7\ B_8]^t$.

Then introducing $Z = 0$ into the previous relations, it follows

$$\{W(Z=0)\} = \begin{bmatrix} \mathbf{X}_c(0) \\ \mathbf{X}_s(0) \\ \mathbf{Y}_c(0) \\ \mathbf{Y}_s(0) \\ 1 \end{bmatrix} = \underset{17\times 17}{[M]} \begin{bmatrix} \mathbf{A} \\ \mathbf{B} \\ 1 \end{bmatrix}. \tag{9}$$

The deflections and their derivatives at $Z = L$ can also be obtained from Eqn (7) and written in the following form

$$\{W(Z=L)\} = \begin{bmatrix} \mathbf{X}_c(L) \\ \mathbf{X}_s(L) \\ \mathbf{Y}_c(L) \\ \mathbf{Y}_s(L) \\ 1 \end{bmatrix} = \underset{17\times 17}{[H]} \begin{bmatrix} \mathbf{A} \\ \mathbf{B} \\ 1 \end{bmatrix}. \tag{10}$$

Combining two Eqns (8) and (9) results in

$$\{W(Z=L)\} = [N]\cdot\{W(Z=0)\} \tag{11}$$

where $[N] = [H]\cdot[M]^{-1}$.

We can also derive the following relations between the derivatives of the displacement functions and the state variables, represented in a matrix form

$$\{W\} = \underset{17\times 17}{[\mathbf{A}]}\ \{S\} \tag{12}$$

where $\{W\} = (X_c, X_c', X_c'', X_c''', X_s, X_s', X_s'', X_s''', Y_c, Y_c', Y_c'', Y_c''', Y_s, Y_s', Y_s'', Y_s''', 1)^t$, $\{S\} = \{X_c, X_s, Y_c, Y_s, \alpha_c, \alpha_s, \beta_c, \beta_s, M_{xc}, M_{xs}, M_{yc}, M_{ys}, Q_{xc}, Q_{xs}, Q_{yc}, Q_{ys}, 1\}^t$ and the elements of matrix $\mathbf{A}$ are referred to by Lee *et al.* [13].

Consider the boundary conditions at $Z = 0$ and $Z = L$, we have

$$\begin{aligned} \{W(Z=L)\} &= [\mathbf{A}]\{S(Z=L)\} = [\mathbf{A}]\{S_l\} \\ \{W(Z=0)\} &= [\mathbf{A}]\{S(Z=0)\} = [\mathbf{A}]\{S_0\}. \end{aligned} \tag{13}$$

The substitution of the above equations into (10) yields

$$\{S_l\} = [\mathbf{A}]^{-1}[\mathbf{N}][\mathbf{A}]\{S_0\} = [\mathbf{T}_s]\{S_0\}. \tag{14}$$

Thus, the transfer matrix $[\mathbf{T}_s]$, with the size of 17×17, is constructed by considering the effects of shaft unbalance to fit the general whirl of the elliptical orbits.

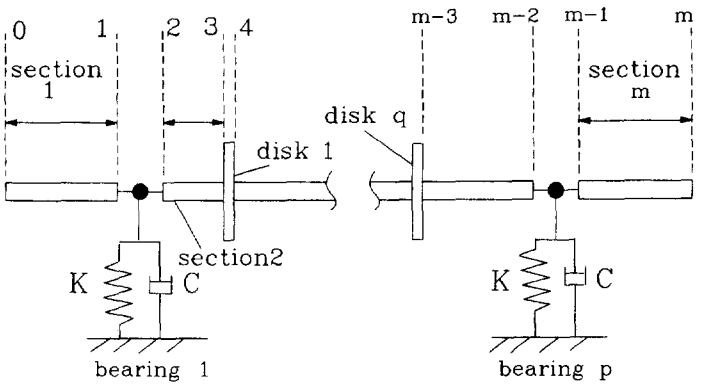

Fig. 2. A general rotor-bearing system.

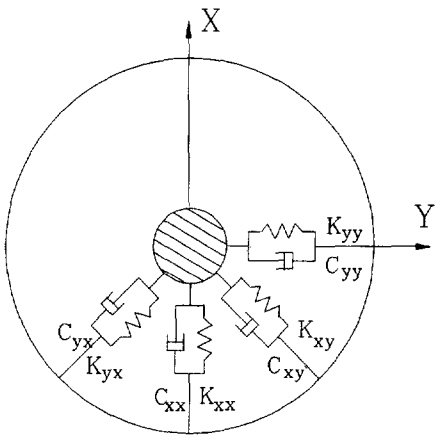

Fig. 3. Model of a bearing.

OVERALL TRANSFER MATRIX FOR THE WHOLE SYSTEM

A typical rotating shaft as shown in Fig. 2 is composed of shafts, disks and bearings. The disks are assumed to be rigid with constant eccentricities and defined by rigid mass elements with gyroscopic effects. From the equilibrium and compatibility conditions, the relations of the state variables between the right side and left side of an unbalance disk is expressed as

$$\begin{bmatrix} \mathbf{S}_r \\ 1 \end{bmatrix} = \underset{17\times 17}{[\mathbf{T}_d]} \begin{bmatrix} \mathbf{S}_l \\ 1 \end{bmatrix}. \tag{15}$$

The dynamic model of the bearings may be simplified as a linear element (see Fig. 3). From the force equilibrium, the relationship of the state variables between the left and right sides can also be obtained as below

$$\begin{bmatrix} \mathbf{S}_r \\ 1 \end{bmatrix} = \underset{17\times 17}{[\mathbf{T}_b]} \begin{bmatrix} \mathbf{S}_l \\ 1 \end{bmatrix}. \tag{16}$$

Details of $[\mathbf{T}_d]$ and $[\mathbf{T}_b]$ are listed in Lee *et al.* [15]. The overall transfer matrix of the system (refer to Fig. 2) is the relation between two free ends of the shaft, which can be derived by relating state variables from one end step by step to another end, or

$$\begin{aligned} \{S_m\} &= [\mathbf{W}]\{S_0\} \\ &= [T_{sm}][T_{bp}][T_{s(m-1)}][T_{dq}], \cdots, [T_{d1}][T_{s2}][T_{b1}][T_{s1}]\{S_0\}. \end{aligned} \tag{17}$$

Because the shear forces and bending moments are zero at both ends, Eqn (16) becomes

$$\begin{bmatrix} \mathbf{S}_m \\ \mathbf{0} \\ 1 \end{bmatrix} = \begin{bmatrix} W_{11} & W_{12} & \mathbf{u}_1 \\ W_{21} & W_{22} & \mathbf{u}_2 \\ 0 & 0 & 1 \end{bmatrix} \begin{bmatrix} \mathbf{S}_0 \\ \mathbf{0} \\ 1 \end{bmatrix} \tag{18}$$

where $\mathbf{S} = [X_c, X_s, Y_c, Y_s, \alpha_c, \alpha_s, \beta_c, \beta_s]^t$, $\mathbf{0} = [0, 0, 0, 0, 0, 0, 0, 0]^t$. The state variables of stages 0 can be solved by Eqn (17) and the state of other stages are obtained by multiplying transfer matrices from stage 0 of left end step by step to the specific stage by using Eqn (16).

FORMULATION FOR UNBALANCE IDENTIFICATION

In the matrix [**F**] of Eqn (7), the first 16 elements of the seventeenth column relating to the particular solutions of the displacement functions are influenced by the unbalance distribution and they can be represented as a linear relationship among the unbalance parameters of the shaft, i.e.

$$\begin{aligned} [F_{1,17}\ F_{2,17}, \ldots, F_{16,17}]^t_{16\times 1} &= [K_1^t \mid K_2^t \mid \cdots \mid K_{16}^t]^t [U_s]_{(4n+2)\times 1} \\ &= [K_f]_{16\times(4n+2)} [U_s]_{(4n+2)\times 1} \end{aligned} \tag{19}$$

where the element of $[K_f]$ are derived in Appendix A. Substituting $Z = L$ into Eqn (18), we obtain the first 16 elements of the seventeenth column in the matrix [**H**] of Eqn (9), or

$$[H_{1,17}\ H_{2,17}, \ldots, H_{16,17}]^t_{16\times 1} = [K_h]_{16\times(4n+2)} [U_s]_{(4n+2)\times 1}. \tag{20}$$

Therefore, the matrix [**H**] can be written into the following form

$$[\mathbf{H}] = \begin{bmatrix} [H_0]_{16\times 16} & [K_h]_{16\times(4n+2)} [U_s]_{(4n+2)\times 1} \\ \underline{0}_{1\times 16} & 1 \end{bmatrix}.$$

Similarly, the first 16 elements of the seventeenth column in the matrix [**M**] of Eqn (8), can also be expressed in the following form by substituting $Z = 0$ into Eqn (18),

$$[M_{1,17}\ M_{2,17}, \ldots, M_{16,17}]^t_{16\times 1} = [K_m]_{16\times(4n+2)} [U_s]_{(4n+2)\times 1}. \tag{21}$$

Then the inverse matrix of [**M**] in Eqn (8) can be written as follows

$$\begin{aligned} [\mathbf{M}]^{-1} &= \begin{bmatrix} [M_0]_{16\times 16} & [K_m]_{16\times(4n+2)} [U_s]_{(4n+2)\times 1} \\ \underline{0}_{1\times 16} & 1 \end{bmatrix} \\ &= \begin{bmatrix} [M_I]_{16\times 16} & [M_u]_{16\times(4n+2)} [U_s]_{(4n+2)\times 1} \\ \underline{0}_{1\times 16} & 1 \end{bmatrix} \end{aligned} \tag{22}$$

where $[M_I] = [M_0]^{-1}$ and $[M_u] = (-1)[M_I][K_m]$. The matrix [**N**] of Eqn (10) can be subsequently obtained as

$$[\mathbf{N}] = [\mathbf{H}][\mathbf{M}]^{-1} = \begin{bmatrix} [N_0]_{16\times 16} & [K_n]_{16\times(4n+2)} [U_s]_{(4n+2)\times 1} \\ \underline{0}_{1\times 16} & 1 \end{bmatrix} \tag{23}$$

where $[N_0] = [H_0][M_I]$, $[K_n] = [H_0][M_u] + [K_h]$. Finally, the matrix [$\mathbf{T}_s$] in Eqn (13), representing the relations of the state variables between the right side and left side of an unbalance shaft, can be obtained as

$$\begin{aligned} [\mathbf{T}_s] &= [\mathbf{A}]^{-1}[\mathbf{N}][\mathbf{A}] \\ &= \begin{bmatrix} [A_0]^{-1}_{16\times 16} & \underline{0}_{16\times 1} \\ \underline{0}_{1\times 16} & 1 \end{bmatrix} \begin{bmatrix} [N_0] & [K_n][U_s] \\ \underline{0} & 1 \end{bmatrix} \begin{bmatrix} [A_0]_{16\times 16} & \underline{0}_{16\times 1} \\ \underline{0}_{1\times 16} & 1 \end{bmatrix} \\ &= \begin{bmatrix} [T_{s0}]_{16\times 16} & [K_s]_{16\times(4n+2)} [U_s]_{(4n+2)\times 1} \\ \underline{0}_{1\times 16} & 1 \end{bmatrix} \end{aligned} \tag{24}$$

where $[T_{s0}] = [A_0]^{-1}[N_0][A_0]$ and $[K_s] = [A_0]^{-1}[K_n]$.

In summary, the transfer matrices of the shaft sections, bearings, and disks, respectively, can be expressed by the following form

$$[\mathbf{T}_{si}] = \begin{bmatrix} [T_{s0i}]_{16\times 16} & [K_{si}]_{16\times(4n+2)}[U_{si}]_{(4n+2)\times 1} \\ \underline{0}_{1\times 16} & 1 \end{bmatrix}$$

$$[\mathbf{T}_{bj}] = \begin{bmatrix} [T_{b0j}]_{16\times 16} & \underline{0}_{16\times 1} \\ \underline{0}_{1\times 16} & 1 \end{bmatrix}$$

$$[\mathbf{T}_{dk}] = \begin{bmatrix} [T_{d0k}]_{16\times 16} & [K_{dk}]_{16\times 2}[U_d]_{2\times 1} \\ \underline{0}_{1\times 16} & 1 \end{bmatrix} \tag{25}$$

where i is the ith element of the shafts, j is the jth element of the bearings, k is the kth element of the disks. $K_{dk(13,1)} = K_{dk(14,1)} = m_d\omega^2$, $K_{dk(15,1)} = K_{dk(16,1)} = -m_d\omega^2$ while the other elements of $[K_{dk}]$ are zero and $[U_d] = [e_{dx}\ e_{dy}]^t$. The overall transfer matrix $[\mathbf{W}]$ in Eqn (16), representing the relations between two free ends of the rotor, can be written as

$$\begin{aligned}[\mathbf{W}] &= [T_{sm}][T_{bp}][T_{s(m-1)}][T_{dq}], \ldots, [T_{d1}][T_{s2}][T_{b1}][T_{s1}] \\ &= \begin{bmatrix} [T_{s0m}][T_{b0p}][T_{s0(m-1)}][T_{d0q}], \ldots, [T_{d01}][T_{s02}][T_{b01}][T_{s01}] & [KK][\mathbf{U}] \\ \underline{0} & 1 \end{bmatrix} \\ &= \begin{bmatrix} [TT]_{16\times 16} & [KK]_{16\times m_1}[U]_{m_1\times 1} \\ \underline{0}_{1\times 16} & 1 \end{bmatrix}\end{aligned} \tag{26}$$

where $m_1 = m(4n + 2) + 2q$, $[KK]$ and $[\mathbf{U}]$ are listed in Appendix B. Substituting Eqn (25) above into Eqn (17), we have

$$\begin{bmatrix} \mathbf{S}_m \\ \mathbf{0} \\ 1 \end{bmatrix} = \begin{bmatrix} \begin{bmatrix} TT_{11} & TT_{12} \\ TT_{21} & TT_{22} \end{bmatrix}_{16\times 16} & \begin{bmatrix} KK_{11} & KK_{12} \\ KK_{21} & KK_{22} \end{bmatrix}_{16\times m_1} [\mathbf{U}]_{m_1\times 1} \\ \underline{0}_{1\times 16} & 1 \end{bmatrix} \begin{bmatrix} \mathbf{S}_0 \\ \mathbf{0} \\ 1 \end{bmatrix}. \tag{27}$$

Eight rows of equations can be extracted from the above equation to show as below

$$\underline{0}_{8\times 8} = [TT_{21}]_{8\times 8}\ \mathbf{S}_0 + [KK_{21}\ K_{22}]_{8\times m_1}[\mathbf{U}]_{m_1\times 1} \tag{28}$$

where $\mathbf{S}_0$ is the state variables of the left free end, or,

$$[\mathbf{CC}]_{8\times m_1}[\mathbf{U}]_{m_1\times 1} = [\mathbf{DD}]_{8\times 1} \tag{29}$$

where $[\mathbf{CC}] = [KK_{21}\ KK_{22}]$, $[\mathbf{DD}] = -[TT_{21}]_{8\times 8}\mathbf{S}_0$. In the above equation, $\mathbf{S}_0$ represents the state vector of both displacements and angles measured at one free end in one shaft.The elements of $[TT_{21}]$ and $[KK_{21}\ KK_{22}]$ are dependent on the system's parameters, such as the geometry shape, the material properties, the rotating speed and so on and $[\mathbf{U}]$ is the parameters representing the unbalance distribution function. This is, $[\mathbf{CC}]$ is a $8\times m_1$ known matrix, $[\mathbf{DD}]$ is a 8×1 known vector and $[\mathbf{U}]$ is a $m_1\times 1$ unknown vector. It can be shown that, for one rotating speed, there are five independent equations available in matrix Eqn (27), which may not be sufficient to solve the unbalance distribution function. In that case, the rotor system must be measured at several different rotating speeds, say k. Then, the equations can be expressed as below

$$\begin{bmatrix} \mathbf{CC}(\omega_1) \\ \cdots\cdots \\ \mathbf{CC}(\omega_2) \\ \cdots\cdots \\ \vdots \\ \mathbf{CC}(\omega_k) \end{bmatrix}_{8k\times m_1} [\mathbf{U}]_{m_1\times 1} = \begin{bmatrix} \mathbf{DD}(\omega_1) \\ \cdots\cdots \\ \mathbf{DD}(\omega_2) \\ \cdots\cdots \\ \vdots \\ \mathbf{DD}(\omega_k) \end{bmatrix}_{8k\times 1} \tag{30}$$

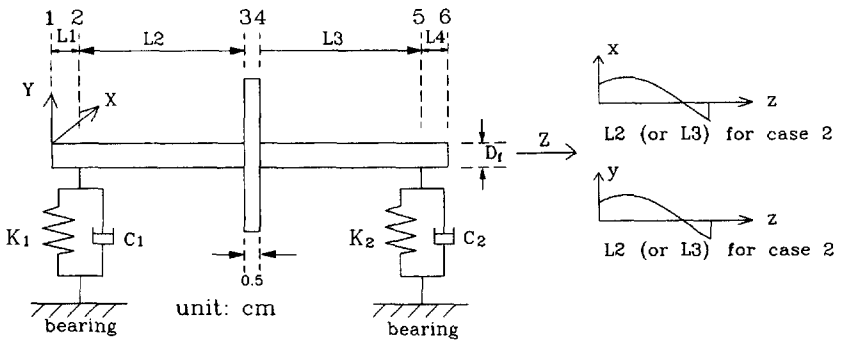

Fig. 4. A rotor-bearing system for numerical cases.

Table 1. The details of case 1

Shaft:
E, G 2.07×10^{11} N/m^2, 8.1×10^{10} N/m^2
ρ, K_s 7750 Kg/m^3, 0.68
$L1 = 1.2$ cm, $L2 = 15$ cm, $L3 = 15$ cm, $L4 = 1.2$ cm
diameters of all the shafts $D_f = 1$ cm
Disk:
diameter of disk 5 cm
disk thick h 0.5 cm
disk mass M_d 0.0761 Kg
Bearing:
$K_{xx}, K_{yy}, K_{xy}, K_{yx}$ 2.0×10^6, 1.5×10^6, 0, 0 N/m
$C_{xx}, C_{yy}, C_{xy}, C_{yx}$ 200, 100, 0, 0 N·s/m
The unbalance of the disk:
$e_{dx} = 0.001$ cm, $e_{dy} = 0.001$ cm.
The unbalance distribution of the shafts:
$L2$ projection in $x - z$ plane ($\phi = 0$ rad)
$r_x(Z) = 0.001$ cm;
projection in $y - z$ plane ($\phi = \pi/2$ rad)
$r_y(Z) = 0.001$ cm;
$L3$ projection in $x - z$ plane ($\phi = 0$ rad)
$r_x(Z) = 0.001$ cm;
projection in $y - z$ plane ($\phi = \pi/2$ rad)
$r_y(Z) = 0.001$ cm;
$L1$ and $L4$ no unbalance.

or

$$[AA]_{8k \times m_1}[\mathbf{U}]_{m_1 \times 1} = [BB]_{8k \times 1}. \tag{31}$$

Consequently, we have $5k$ independent equations to solve for the m_1 unknowns and it will yield the estimated coefficient of $[\mathbf{U}]$ by using least squares method only if we choose a suitable k such that

$$5k \geqslant m_1. \tag{32}$$

Specifically, multiplying the matrix $[\mathbf{AA}]^t$ at both sides of Eqn (30) simultaneously, we have

$$[EE]_{m_1 \times m_1}[\mathbf{U}] = [FF]_{m_1 \times 1} \tag{33}$$

where $[EE] = [\mathbf{AA}]^t[\mathbf{AA}]$, $[FF] = [\mathbf{AA}]^t[BB]$ and the parameters of the unbalance distribution function acquired are obtained by the following equation,

$$[\mathbf{U}]_{m_1 \times 1} = [EE]^{-1}_{m_1 \times m_1}[FF]_{m_1 \times 1}. \tag{34}$$

Table 2. The details of case 2

The unbalance of the disk:
$e_{dx} = 0.001$ cm, $e_{dy} = 0.001$ cm.
The unbalance distribution of the shafts:
$L2$ $r_x(Z) = 0.001 \cdot \cos(\pi z/L2) + 0.001 \cdot \sin(\pi z/L2)$
$r_y(Z) = 0.001 \cdot \cos(\pi z/L2) + 0.001 \cdot \sin(\pi z/L2)$;
$L3$ $r_x(Z) = 0.001 \cdot \cos(\pi z/L3) + 0.001 \cdot \sin(\pi z/L3)$
$r_y(Z) = 0.001 \cdot \cos(\pi z/L3) + 0.001 \cdot \sin(\pi z/L3)$;
$L1$ and $L4$ no unbalance.

Table 3. The details of case 3

The unbalance of the disk:
$e_{dx} = 0.001$ cm, $e_{dy} = 0.001$ cm.
The unbalance distribution of the shafts:
$L2$ $r_x(Z) = 0.001 \cdot \sin(\pi z/L2)$
$r_y(Z) = -0.001 \cdot \sin(\pi z/L2)$;
$L3$ $r_x(Z) = 0.001 \cdot \sin(\pi z/L3)$
$r_y(Z) = 0.001 \cdot \sin(\pi z/L3)$;
$L1$ and $L4$ no unbalance.

Table 4. The numerical results of case 1

		Exact	$\omega_1 - \omega_2 (n = 2)$	$\omega_1 - \omega_3 (n = 3)$	$\omega_1 - \omega_4 (n = 4)$	$\omega_1 - \omega_5 (n = 5)$
Disk	e_{dx}	0.001	9.99904×10^{-4}	9.99908×10^{-4}	9.99906×10^{-4}	9.99904×10^{-4}
	e_{dy}	0.001	9.99910×10^{-4}	9.99912×10^{-4}	9.99910×10^{-4}	9.99911×10^{-4}
$L2$	constant term in x-z plane	0.001	9.99937×10^{-4}	9.99936×10^{-4}	9.99955×10^{-4}	9.99962×10^{-4}
	constant term in y-z plane	0.001	9.99969×10^{-4}	9.99965×10^{-4}	9.99971×10^{-4}	9.99977×10^{-4}
$L3$	constant term in x-z plane	0.001	9.99936×10^{-4}	9.99937×10^{-4}	9.99950×10^{-4}	9.99957×10^{-4}
	constant term in y-z plane	0.001	9.99968×10^{-4}	9.99952×10^{-4}	9.99967×10^{-4}	9.99973×10^{-4}
Average error (%)		—	6.2667×10^{-3}	6.5×10^{-3}	5.683×10^{-3}	5.2667×10^{-3}

(unit: cm)
The measurement speeds $\omega_1, \omega_2, \ldots, \omega_5$ are chosen as 117, 188, 292, 362, 487 (rpm).

Table 5. The numerical results of case 2

			Exact	$\omega_1 - \omega_3 (n = 3)$	$\omega_1 - \omega_4 (n = 4)$	$\omega_1 - \omega_5 (n = 5)$	$\omega_1 - \omega_6 (n = 6)$
Disk		e_{dx}	0.001	1.19157×10^{-3}	1.07264×10^{-3}	1.01795×10^{-3}	1.00236×10^{-3}
		e_{dy}	0.001	1.08155×10^{-3}	9.95921×10^{-4}	9.93450×10^{-4}	9.99738×10^{-4}
$L2$		constant	0	-2.2498×10^{-4}	-8.5479×10^{-5}	-2.1201×10^{-5}	-2.8527×10^{-6}
	x-z	$\cos(\pi z/L2)$	0.001	1.14877×10^{-3}	1.05655×10^{-3}	1.01403×10^{-3}	1.00189×10^{-3}
		$\sin(\pi z/L2)$	0.001	1.23374×10^{-3}	1.08878×10^{-3}	1.02202×10^{-3}	1.00296×10^{-3}
		constant	0	-9.4315×10^{-5}	5.04926×10^{-6}	7.78023×10^{-6}	3.05806×10^{-7}
	y-z	$\cos(\pi z/L2)$	0.001	1.06212×10^{-3}	9.96614×10^{-4}	9.94842×10^{-4}	9.99798×10^{-4}
		$\sin(\pi z/L2)$	0.001	1.09824×10^{-3}	9.94804×10^{-4}	9.91931×10^{-4}	9.99682×10^{-4}
$L3$		constant	0	-1.9626×10^{-4}	-7.3539×10^{-5}	-1.7864×10^{-5}	-2.1886×10^{-6}
	x-z	$\cos(\pi z/L3)$	0.001	8.37735×10^{-4}	9.38702×10^{-4}	9.84932×10^{-4}	9.98059×10^{-4}
		$\sin(\pi z/L3)$	0.001	1.17307×10^{-3}	1.06437×10^{-3}	1.01547×10^{-3}	1.00180×10^{-3}
		constant	0	-9.1318×10^{-5}	2.70404×10^{-6}	6.19849×10^{-6}	2.25970×10^{-7}
	y-z	$\cos(\pi z/L3)$	0.001	9.28883×10^{-4}	1.00306×10^{-3}	1.00541×10^{-3}	1.00020×10^{-3}
		$\sin(\pi z/L3)$	0.001	1.08474×10^{-3}	9.98411×10^{-4}	9.94806×10^{-4}	9.99818×10^{-4}
Average error (%)			—	13.672%	3.7967%	1.1997%	0.1264%

(unit: cm)
The measurement speeds $\omega_1, \omega_2, \ldots, \omega_6$ are chosen as 9560, 9580, 9640, 9700, 11000, 12000 (rpm).

NUMERICAL EXAMPLES

In this section, three numerical examples are presented to illustrate the feasibility and applicability of the proposed method. As shown in Fig. 4, a rotor system with separately-mounted bearings near the free ends is given. It is assumed that only the two central elements of the shafts (i.e. $L2$ and $L3$) and the disk, are unbalanced. The differences among the three cases are the unbalance distributions of the shafts, details of which are listed in Tables 1–3. In case 1, all shaft unbalances are assumed to be uniform. There are six unbalance parameters to be estimated for the disk and the shafts in this case. By Eqn (31), we at least need to measure two rotating speeds ($k \geqslant 2$) to estimate the six parameters. Arbitrary simulated speeds are chosen for $k = 2 - k = 5$ and listed in Table 4 along with simulation results. This table shows that good results are obtained where the average error ranges from 0.00527% to 0.0065%. In case 2, the spatial unbalance distribution curve is specified, i.e. two terms of the Fourier series representation of the unbalance distribution of the shaft projected

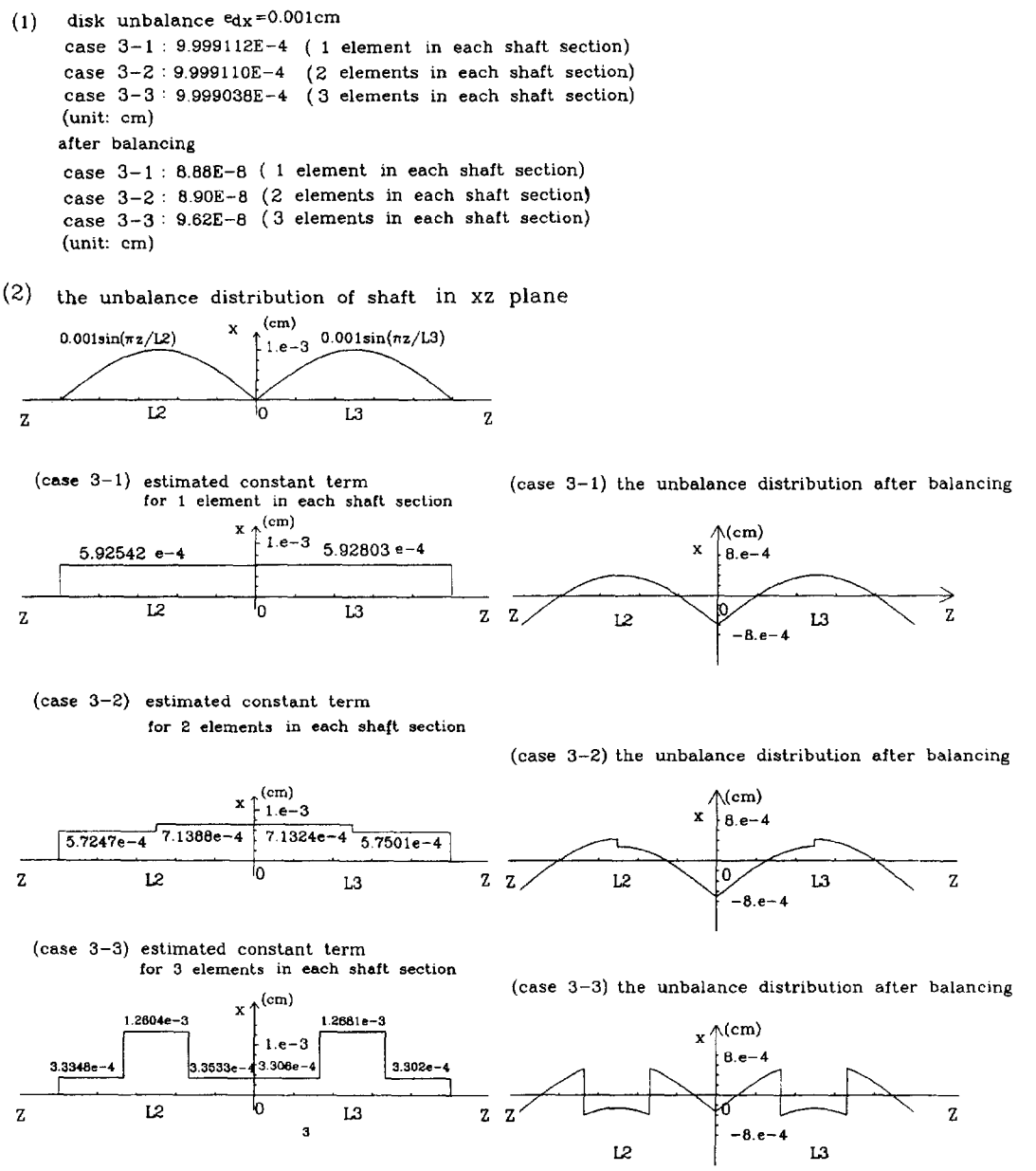

Fig. 5. (a) The estimated unbalance distributions before and after balancing in xz plane in case 3; (b) The estimated unbalance distributions before and after balancing in yz plane in case 3; (c) The comparisons of the disk responses between original and balanced system in case 3.

(1) disk unbalance e_{dy} =0.001cm

case 3-1: 9.999092e-4 (1 element in each shaft section)
case 3-2: 9.999040e-4 (2 elements in each shaft section)
case 3-3: 9.999043e-4 (3 elements in each shaft section)
(unit: cm)
after balancing
case 3-1: 9.08e-8 (1 element in each shaft section)
case 3-2: 9.60e-8 (2 elements in each shaft section)
case 3-3: 9.57e-8 (3 elements in each shaft section)
(unit: cm)

(2) the unbalance distribution of shaft in yz plane

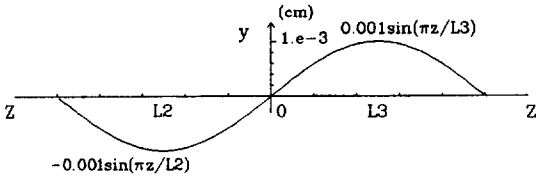

(case 3-1) estimated constant term for 1 element in each shaft section

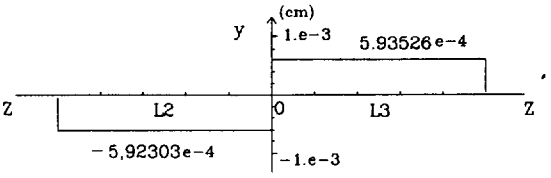

(case 3-1) the unbalance distribution after balancing

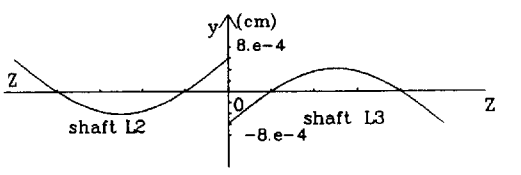

(case 3-2) estimated constant term for 2 elements in each shaft section

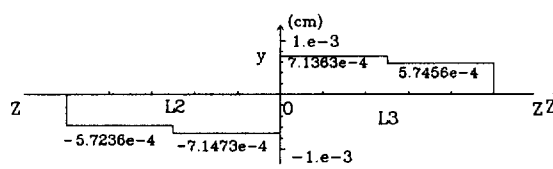

(case 3-2) the unbalance distribution after balancing

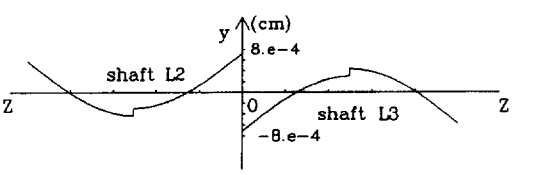

(case 3-3) estimated constant term for 3 elements in each shaft section

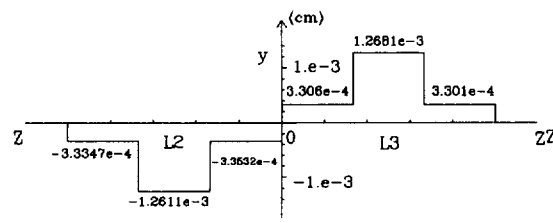

(case 3-3) the unbalance distribution after balancing

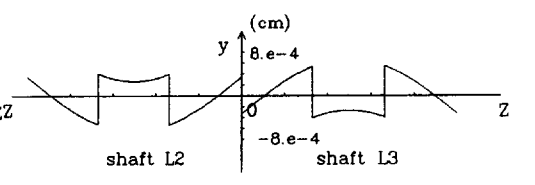

Fig. 5. (continued).

onto the XZ and YZ planes are given (see Fig. 4). In all, we have 14 variables to be estimated and by Eqn (31), we need at least three spin speeds. Three–six is used for the value of k in Eqn (31) and the results are shown in Table 5. The simulation results show there is a 13.672% average error when $k = 3$. When k is increased to 6, the average error is reduced to 0.1264% and good results are obtained.

In general, balancing is effected by adding weights or digging holes at given radial distances from the axis of rotation. Therefore, case 3 is focused on estimating the constant-term coefficients of the shafts and disk without *a priori* information about unbalance. The actual unbalance distribution of the shafts is assumed to be a sine waveform (see Table 3). In this case, we choose $k = 6$ and have the same rotating speeds as Table 2. Each shaft is considered as having one to three sections to investigate the effectiveness of balancing. The simulation results are shown in Figs 5(a, b). Comparisons of the responses before balancing and after balancing, are displayed in four curves in Fig. 5(c). Owing to the gyroscopic effect at high speeds, the first critical response is split into two peaks at 9580

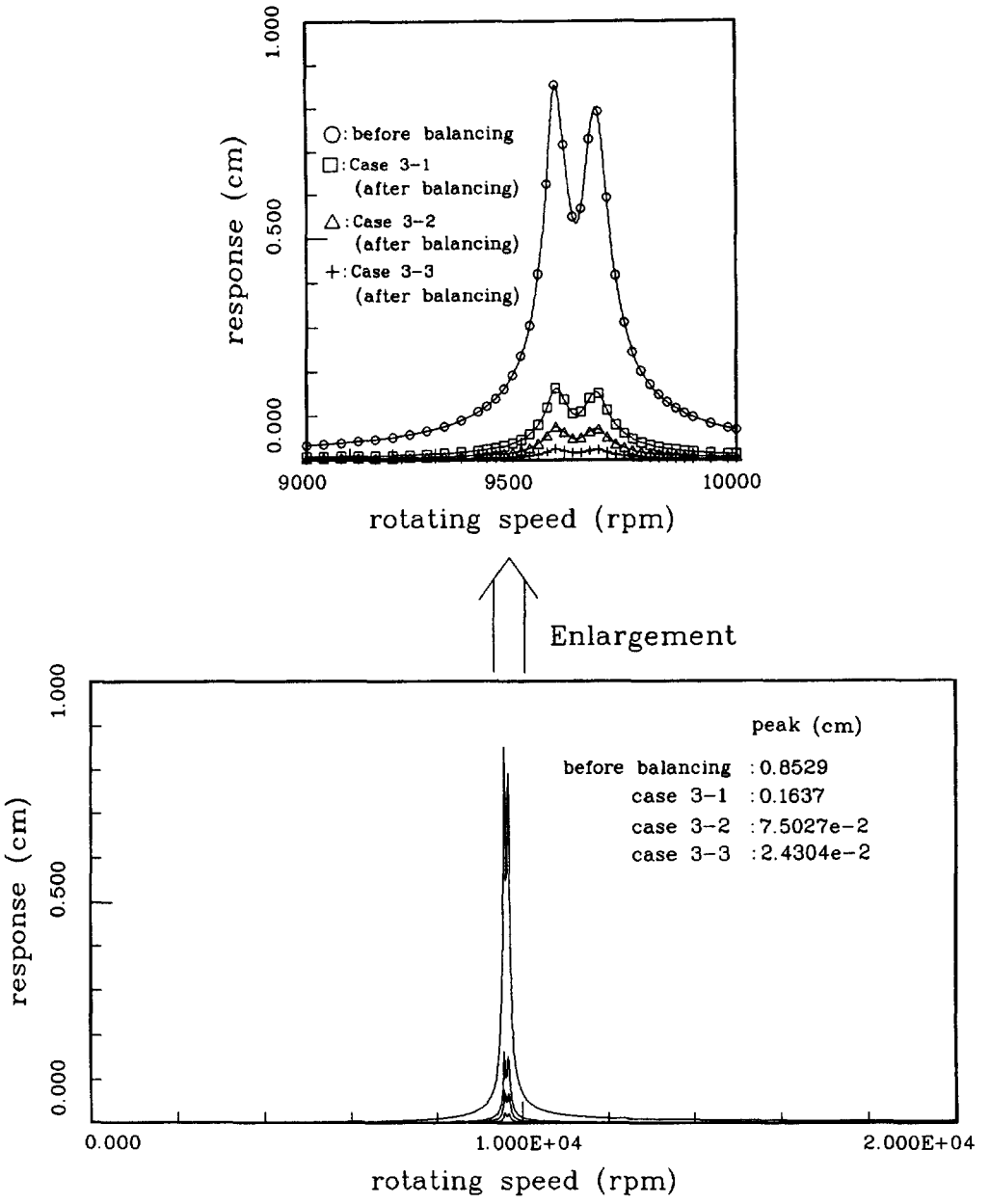

Fig. 5. (continued).

and 9680 rpm. It is noted that the peak response is not proportional to the net integrated area of unbalance distribution because the effects of unbalances at different locations on the response are not equal. From this figure, we find that the peak response in case 3–1 is about 19.193% of the original response before balancing. When one shaft is divided into three sections, the peak response is reduced to 2.850% of the original peak and it shows a good balance.

A more complex rotor-bearing system in which the shaft has distinct diameters can be considered in the same manner; the shaft can be cut into several sections and the solution obtained.

CONCLUSION

Balancing plays an important role in rotating machinery, especially in high-speed rotor-bearing systems. If the exact unbalance distribution can be found, then better balancing can be achieved. In the past, before Lee *et al.* [13], there was no method for describing the continuous "state of unbalance" in a flexible rotor shaft. This is the first paper to propose a theoretical model and

estimation technique for finding the unbalance distribution function in a rotor shaft. Three simple numerical cases are given and good approximations are obtained. It may be a new start for achieving the better balance in actual systems in the future.

Acknowledgements—This study was supported by the National Science Council, Republic of China, under contract number NSC 81-0401-E-009-08.

REFERENCES

1. Bishop, R. E. D. and Gladwell, G. M. L., The vibration and balancing of an unbalanced rotor. *Journal of Mechanical Engineering Science*, 1959, **1**(1) 66–77.
2. Kellenberger, W., Should a flexible rotor be balanced in n or $(n + 2)$ planes? *ASME Journal of Engineering for Industry*, 1972, **94**(2) 548–560.
3. Shimada, K. and Miwa, S., Balancing of a flexible rotor. *Bulletin of the JSME*, 1980, **23**(180) 938–944.
4. Shimada, K. Fujisawa, F., Balancing method of multi-span, multi-bearings rotor system. *Bulletin of the JSME*, 1980, **23**(185) 1894–1898.
5. Saito, S. and Azuma, T., Balancing of flexible rotors by the complex modal method. *ASME Journal of Vibration, Acoustics, Stress and Reliability in Design*, 1983, **105**, 94–100.
6. Goodman, T. P., A least-squares method for computing balance corrections. *ASME Journal of Engineering for Industry, Series B*, 1964, **86**(3) 273–279.
7. Lund, J. W. and Tonnesen, J., Analysis and experiments on multi-plane balancing of a flexible rotor. *ASME Journal of Engineering for Industry*, 1972, 233–242.
8. Tessarzik, J. M. and Badgley, R. H., Experimental evaluation of the exact point-speed and least-squares procedures for flexible rotor balancing by the influence coefficient method. *ASME Journal of Engineering for Industry, Series B*, 1974, **96**(2) 633–643
9. Tessarzik, J. M., Badgley, R. H. and Anderson, W. J., Flexible rotor balancing by the exact point-speed influence coefficient method. *ASME Journal of Engineering for Industry, Series B*, 1972, **94**(1) 148–158.
10. Tessarzik, J. M., Badgley, R. H. and Fleming, D. P., Experimental evaluation of multiplane-multispeed rotor balancing through multiple critical speeds. *ASME Journal of Engineering for Industry*, 1976, 988–998.
11. Everett, L. J., Two-plane balancing of a rotor system without phase response measurements. *ASME Journal of Vibration, Acoustics, Stress and Reliability in Design*, 1987, **109**, 162–167.
12. Ehrich, F. F., Handbook of Rotordynamics. McGraw-Hill, New York, 1992.
13. Lee, A. C., Shih, Y. P. and Kang Y., The analysis of linear rotor-bearing systems: a general transfer matrix method. *ASME Journal of Vibration and Acoustics*, 1993, **115**, 490–497.
14. Wylie, C. R. and Barrett, L. C., *Advanced Engineering Mathematics*. McGraw-Hill, New York, 1982, Chapter 7.
15. Lee, A. C., Kang, Y. and Liu, S. L., A modified transfer matrix method for the linear rotor-bearing system. *ASME Journal of Applied Mechanics*, 1991, **58**, 776–783.

APPENDIX A

$$F_{1,17} = X_c^p = \zeta_{10} + \sum_{n=1}^{\infty} \left(\mu_{cn}^c \cdot \cos \frac{n\pi Z}{L} + \mu_{cn}^s \cdot \sin \frac{n\pi Z}{L} \right) = [P_1][V_1]$$

$$F_{2,17} = (F_{1,17})' = [P_2][V_1]$$

$$F_{3,17} = (F_{2,17})' = [P_3][V_1]$$

$$F_{4,17} = (F_{3,17})' = [P_4][V_1]$$

$$F_{5,17} = X_s^p = [P_1][V_2]$$

$$F_{6,17} = (F_{5,17})' = [P_2][V_2]$$

$$F_{7,17} = (F_{6,17})' = [P_3][V_2]$$

$$F_{8,17} = (F_{7,17})' = [P_4][V_2]$$

$$F_{9,17} = Y_c^p = [P_1][V_3]$$

$$F_{10,17} = (F_{9,17})' = [P_2][V_3]$$

$$F_{11,17} = (F_{10,17})' = [P_3][V_3]$$

$$F_{12,17} = (F_{11,17})' = [P_4][V_3]$$

$$F_{13,17} = Y_s^p = [P_1][V_4]$$

$$F_{14,17} = (F_{13,17})' = [P_2][V_4]$$

$$F_{15,17} = (F_{14,17})' = [P_3][V_4]$$

$$F_{16,17} = (F_{15,17})' = [P_4][V_4] \tag{A1}$$

where

$$[P_1]=\left[1\ \cos\frac{\pi z}{L}\ \sin\frac{\pi z}{L},\ldots,\cos\frac{n\pi z}{L}\ \sin\frac{n\pi z}{L}\right]$$

$$[P_2]=\left[0\ -\frac{\pi}{L}\sin\frac{\pi z}{L}\ \frac{\pi}{L}\cos\frac{\pi z}{L},\ldots,-\frac{n\pi}{L}\sin\frac{n\pi z}{L}\ \frac{n\pi}{L}\cos\frac{n\pi z}{L}\right]$$

$$[P_3]=\left[0\ -\left(\frac{\pi}{L}\right)^2\cos\frac{\pi z}{L}\ -\left(\frac{\pi}{L}\right)^2\sin\frac{\pi z}{L},\ldots,-\left(\frac{n\pi}{L}\right)^2\cos\frac{n\pi z}{L}\ -\left(\frac{n\pi}{L}\right)^2\sin\frac{n\pi z}{L}\right]$$

$$[P_4]=\left[0\ \left(\frac{\pi}{L}\right)^3\sin\frac{\pi z}{L}\ -\left(\frac{\pi}{L}\right)^3\cos\frac{\pi z}{L},\ldots,\left(\frac{n\pi}{L}\right)^3\sin\frac{n\pi z}{L}\ -\left(\frac{n\pi}{L}\right)^3\cos\frac{n\pi z}{L}\right]$$

$$[V_1]=[\zeta_{10}\ \mu_{c1}^c\ \mu_{c1}^s,\ldots,\mu_{cn}^c\ \mu_{cn}^s]^t,\quad [V_2]=[\zeta_{20}\ \mu_{s1}^c\ \mu_{s1}^s,\ldots,\mu_{sn}^c\ \mu_{sn}^s]^t$$

$$[V_3]=[\zeta_{30}\ v_{c1}^c\ v_{c1}^s,\ldots,v_{cn}^c\ v_{cn}^s]^t,\quad [V_4]=[\zeta_{40}\ v_{s1}^c\ v_{s1}^s,\ldots,v_{sn}^c\ v_{sn}^s]^t.$$

The relations between the nth term of the Fourier series representing the unbalance function (see Eqn (3)) and the nth term of the particular solution in Eqn (6) can be obtained as below

$$\begin{bmatrix}\mu_{cn}^c\\ \mu_{cn}^s\\ \mu_{sn}^c\\ \mu_{sn}^s\\ v_{cn}^c\\ v_{cn}^s\\ v_{sn}^c\\ v_{sn}^s\end{bmatrix}=\sigma_n\cdot\begin{bmatrix}A_n&0&0&0&0&C_n&-B_n&0\\ 0&A_n&0&0&-C_n&0&0&-B_n\\ 0&0&A_n&0&B_n&0&0&C_n\\ 0&0&0&A_n&0&B_n&-C_n&0\\ 0&-C_n&B_n&0&A_n&0&0&0\\ C_n&0&0&B_n&0&A_n&0&0\\ -B_n&0&0&-C_n&0&0&A_n&0\\ 0&-B_n&C_n&0&0&0&0&A_n\end{bmatrix}^{-1}\begin{bmatrix}r_{cn}\cos\phi\\ r_{sn}\cos\phi\\ -r_{cn}\sin\phi\\ -r_{sn}\sin\phi\\ r_{cn}\sin\phi\\ r_{sn}\sin\phi\\ r_{cn}\cos\phi\\ r_{sn}\cos\phi\end{bmatrix}$$

$$=\begin{bmatrix}a_{11})_n&a_{12})_n\\ a_{21})_n&a_{22})_n\\ a_{31})_n&a_{32})_n\\ a_{41})_n&a_{42})_n\\ a_{51})_n&a_{52})_n\\ a_{61})_n&a_{62})_n\\ a_{71})_n&a_{72})_n\\ a_{81})_n&a_{82})_n\end{bmatrix}\begin{bmatrix}r_{cn}\\ r_{sn}\end{bmatrix}\tag{A2}$$

where

$$\sigma_n=\frac{\rho\cdot A\cdot\omega^2}{EI}+\frac{\rho\omega^2}{K_sG}\left(\frac{n\pi}{L}\right)^2-\frac{\rho^2\omega^4}{K_sGE}+\frac{2\rho^2\omega^4}{K_sGE},\quad c=\frac{T}{EI},\quad d=\frac{T\rho\omega^2}{EIK_sG},$$

$$f_1=\frac{\rho\omega^2}{E}+\frac{\rho\omega^2}{K_sG}-\frac{P}{EI},\quad g=\frac{\rho^2\omega^4}{K_sGE}-\frac{\rho\cdot A\cdot\omega^2}{EI},\quad h=\frac{2\rho\omega^2}{E},\quad k=\frac{2\rho^2\omega^4}{K_sGE},$$

$$A_n=\left(\frac{n\pi}{L}\right)^4-f_1\left(\frac{n\pi}{L}\right)^2+g,\quad B_n=-h\left(\frac{n\pi}{L}\right)^2+k,\quad C_n=d\left(\frac{n\pi}{L}\right)-c\left(\frac{n\pi}{L}\right)^3.$$

By substituting $n=1$ to $n=n$ into the above equation, those equations can be rearranged into the following four forms

$$\begin{bmatrix}\zeta_{10}\\ \mu_{c1}^c\\ \mu_{c1}^s\\ \mu_{c2}^c\\ \mu_{c2}^s\\ \vdots\\ \mu_{cn}^c\\ \mu_{cn}^s\end{bmatrix}=\begin{bmatrix}c_1&0&0&0&0&\cdots&0&0\\ 0&a_{11})_1&a_{12})_1&0&0&\cdots&0&0\\ 0&a_{21})_1&a_{22})_1&0&0&\cdots&0&0\\ 0&0&0&a_{11})_2&a_{12})_2&\cdots&0&0\\ 0&0&0&a_{21})_2&a_{22})_2&\cdots&0&0\\ \vdots&\vdots&\vdots&\vdots&\vdots&\cdots&\vdots&\vdots\\ 0&0&0&0&0&\cdots&a_{11})_n&a_{12})_n\\ 0&0&0&0&0&\cdots&a_{21})_n&a_{22})_n\end{bmatrix}\begin{bmatrix}r_0\\ r_{c1}\\ r_{s1}\\ r_{c2}\\ r_{s2}\\ \vdots\\ r_{cn}\\ r_{sn}\end{bmatrix}$$

$$\begin{bmatrix} \zeta_{20} \\ \mu_{s1}^{c} \\ \mu_{s1}^{s} \\ \mu_{s2}^{c} \\ \mu_{s2}^{s} \\ \vdots \\ \mu_{sn}^{c} \\ \mu_{sn}^{s} \end{bmatrix} = \begin{bmatrix} c_2 & 0 & 0 & 0 & 0 & \cdots & 0 & 0 \\ 0 & a_{31})_1 & a_{32})_1 & 0 & 0 & \cdots & 0 & 0 \\ 0 & a_{41})_1 & a_{42})_1 & 0 & 0 & \cdots & 0 & 0 \\ 0 & 0 & 0 & a_{31})_2 & a_{32})_2 & \cdots & 0 & 0 \\ 0 & 0 & 0 & a_{41})_2 & a_{42})_2 & \cdots & 0 & 0 \\ \vdots & \vdots & \vdots & \vdots & \vdots & \cdots & \vdots & \vdots \\ 0 & 0 & 0 & 0 & 0 & \cdots & a_{31})_n & a_{32})_n \\ 0 & 0 & 0 & 0 & 0 & \cdots & a_{41})_n & a_{42})_n \end{bmatrix} \begin{bmatrix} r_0 \\ r_{c1} \\ r_{s1} \\ r_{c2} \\ r_{s2} \\ \vdots \\ r_{cn} \\ r_{sn} \end{bmatrix}$$

$$\begin{bmatrix} \zeta_{30} \\ v_{c1}^{c} \\ v_{c1}^{s} \\ v_{c2}^{c} \\ v_{c2}^{s} \\ \vdots \\ v_{cn}^{c} \\ v_{cn}^{s} \end{bmatrix} = \begin{bmatrix} c_3 & 0 & 0 & 0 & 0 & \cdots & 0 & 0 \\ 0 & a_{51})_1 & a_{52})_1 & 0 & 0 & \cdots & 0 & 0 \\ 0 & a_{61})_1 & a_{62})_1 & 0 & 0 & \cdots & 0 & 0 \\ 0 & 0 & 0 & a_{51})_2 & a_{52})_2 & \cdots & 0 & 0 \\ 0 & 0 & 0 & a_{61})_2 & a_{62})_2 & \cdots & 0 & 0 \\ \vdots & \vdots & \vdots & \vdots & \vdots & \cdots & \vdots & \vdots \\ 0 & 0 & 0 & 0 & 0 & \cdots & a_{51})_n & a_{52})_n \\ 0 & 0 & 0 & 0 & 0 & \cdots & a_{61})_n & a_{62})_n \end{bmatrix} \begin{bmatrix} r_0 \\ r_{c1} \\ r_{s1} \\ r_{c2} \\ r_{s2} \\ \vdots \\ r_{cn} \\ r_{sn} \end{bmatrix}$$

$$\begin{bmatrix} \zeta_{40} \\ v_{s1}^{c} \\ v_{s1}^{s} \\ v_{s2}^{c} \\ v_{s2}^{s} \\ \vdots \\ v_{sn}^{c} \\ v_{sn}^{s} \end{bmatrix} = \begin{bmatrix} c_4 & 0 & 0 & 0 & 0 & \cdots & 0 & 0 \\ 0 & a_{71})_1 & a_{72})_1 & 0 & 0 & \cdots & 0 & 0 \\ 0 & a_{81})_1 & a_{82})_1 & 0 & 0 & \cdots & 0 & 0 \\ 0 & 0 & 0 & a_{71})_2 & a_{72})_2 & \cdots & 0 & 0 \\ 0 & 0 & 0 & a_{81})_2 & a_{82})_2 & \cdots & 0 & 0 \\ \vdots & \vdots & \vdots & \vdots & \vdots & \cdots & \vdots & \vdots \\ 0 & 0 & 0 & 0 & 0 & \cdots & a_{71})_n & a_{72})_n \\ 0 & 0 & 0 & 0 & 0 & \cdots & a_{81})_n & a_{82})_n \end{bmatrix} \begin{bmatrix} r_0 \\ r_{c1} \\ r_{s1} \\ r_{c2} \\ r_{s2} \\ \vdots \\ r_{cn} \\ r_{sn} \end{bmatrix}$$

where

$$c_1 = \frac{1}{g}\left(\frac{\rho \cdot A \cdot \omega^2 \cdot \cos\phi}{EI} + \frac{\rho^2 \cdot \omega^4 \cdot \cos\phi}{K_s GE}\right)$$

$$c_2 = \frac{1}{g}\left(\frac{-\rho \cdot A \cdot \omega^2 \cdot \sin\phi}{EI} - \frac{\rho^2 \cdot \omega^4 \cdot \sin\phi}{K_s GE}\right)$$

$$c_3 = \frac{1}{g}\left(\frac{\rho \cdot A \cdot \omega^2 \cdot \sin\phi}{EI} + \frac{\rho^2 \cdot \omega^4 \cdot \sin\phi}{K_s GE}\right)$$

$$c_4 = \frac{1}{g}\left(\frac{\rho \cdot A \cdot \omega^2 \cdot \cos\phi}{EI} + \frac{\rho^2 \cdot \omega^4 \cdot \cos\phi}{K_s GE}\right).$$

For simplicity, the above four equations can be written as below

$$\begin{aligned} [V_1] &= [Y_1][U_s] \\ [V_2] &= [Y_2][U_s] \\ [V_3] &= [Y_3][U_s] \\ [V_4] &= [Y_4][U_s] \end{aligned} \tag{A3}$$

where $[U_s] = [r_0 \ r_{c1} \ r_{s1} \ r_{c2} \ r_{s2}, \ \ldots, \ r_{cn} \ r_{sn}]^t$.

Introducing (A3) into Eqn (A1), the elements of $[K_f]$ can be acquired.

APPENDIX B

$$[T_{b1}][T_{s1}] = \begin{bmatrix} [T_{b01}]_{16\times 16} & \underline{0}_{16\times 1} \\ \underline{0}_{1\times 16} & 1 \end{bmatrix} \begin{bmatrix} [T_{s01}]_{16\times 16} & [K_{s1}]_{16\times(4n+2)}[U_{s1}]_{(4n+2)\times 1} \\ \underline{0}_{1\times 16} & 1 \end{bmatrix}$$

$$= \begin{bmatrix} [T_{b01}]_{16\times 16}[T_{s01}]_{16\times 16} & [T_{b01}]_{16\times 16}[K_{s1}]_{16\times(4n+2)}[U_{s1}]_{(4n+2)\times 1} \\ \underline{0}_{1\times 16} & 1 \end{bmatrix}$$

Successively, we have

$$[T_{s2}][T_{b1}][T_{s1}] = \begin{bmatrix} [T_{s02}]_{16\times 16} & [K_{s2}]_{16\times(4n+2)}[U_{s2}]_{(4n+2)\times 1} \\ \underline{0}_{1\times 16} & 1 \end{bmatrix} \begin{bmatrix} [T_{b01}][T_{s01}] & [T_{b01}][K_{s1}][U_{s1}] \\ \underline{0} & 1 \end{bmatrix}$$

$$= \begin{bmatrix} [T_{s02}][T_{b01}][T_{s01}] & [S_3][Z_3] \\ \underline{0}_{1\times 16} & 1 \end{bmatrix}$$

where

$$[S_3]_{16\times(8n+4)} = [[T_{s02}]_{16\times 16}[T_{b01}]_{16\times 16}[K_{s1}]_{16\times(4n+2)} \vdots [K_{s2}]_{16\times(4n+2)}]$$

$$[Z_3]_{(8n+4)\times 1} = [[U_{s1}]^t_{(4n+2)\times 1} \vdots [U_{s2}]^t_{(4n+2)\times 1}]^t$$

and

$$[T_{d1}][T_{s2}][T_{b1}][T_{s1}] = \begin{bmatrix} [T_{d01}]_{16\times 16} & [K_{d1}]_{16\times 2}[U_{d1}]_{2\times 1} \\ \underline{0}_{1\times 16} & 1 \end{bmatrix} \begin{bmatrix} [T_{s02}][T_{b01}][T_{s01}] & [S_3][Z_3] \\ \underline{0} & 1 \end{bmatrix}$$

$$= \begin{bmatrix} [T_{d01}][T_{s02}][T_{b01}][T_{s01}] & [S_4][Z_4] \\ \underline{0} & 1 \end{bmatrix}$$

where

$$[S_4]_{16\times(8n+4+2)} = [[T_{d01}][T_{s02}][T_{b01}][K_{s1}]_{16\times(4n+2)} \vdots [T_{d01}][K_{s2}]_{16\times(4n+2)} \vdots [K_{d1}]_{16\times 2}]$$

$$[Z_4]_{(12n+6)\times 1} = [[U_{s1}]^t_{(4n+2)\times 1} \vdots [U_{s2}]^t_{(4n+2)\times 1} \vdots [U_{d1}]_{2\times 1}]^t.$$

Then,

$$[T_{sm}][T_{bp}][T_{s(m-1)}][T_{dq}], \ldots, [T_{d1}][T_{s2}][T_{b1}][T_{s1}]$$

$$= \begin{bmatrix} [T_{s0m}][T_{b0p}][T_{s0(m-1)}], \ldots, [T_{s02}][T_{b01}][T_{s01}] & [\mathbf{KK}][\mathbf{U}] \\ \underline{0} & 1 \end{bmatrix}$$

where $m_1 = m(4n + 2) + 2q$,

$$[\mathbf{KK}]_{16\times m_1} = [[T_{s0m}][T_{b0p}][T_{s0(m-1)}][T_{d0q}], \ldots, [T_{d1}][T_{s02}][T_{b01}][K_{s1}]_{16\times(4n+2)} \vdots$$
$$\times [T_{s0m}][T_{b0p}][T_{s0(m-1)}][T_{d0q}], \ldots, [T_{d1}][T_{s03}][K_{s2}]_{16\times(4n+2)} \vdots$$
$$\times [T_{s0m}][T_{b0p}][T_{s0(m-1)}][T_{d0q}], \ldots, [K_{d1}]_{16\times 2} \vdots \cdots \vdots$$
$$\times [T_{s0m}][T_{b0p}][T_{s(m-1)}][K_{dq}]_{16\times 2} \vdots$$
$$\times \vdots [T_{s0m}][T_{b0p}][K_{s(m-1)}]_{16\times(4n+2)} \vdots [K_{sm}]_{16\times(4n+2)}],$$

and

$$[U]_{(m(4n+2)+2q)\times 1} = [[U_{s1}]^t \vdots [U_{s2}]^t \vdots [U_{d1}]^t \vdots, \ldots, \vdots [U_{dq}]^t \vdots [U_{s(m-1)}]^t \vdots [U_{sm}]^t]^t$$